Response to Comments from Anonymous Referee #1

Comments to the Author (General comments): In this paper, the impact of dust chemistry on regional air quality is studied deeply from a super dust storm on March 2010, especially the differences of the two paths. What's more, this study also highlight that the dust also can enhance the heterogeneous reactions, resulting high pollutions, different from the previous study that the dust has a clean effect on the local pollutants. I'm interesting to see this paper published before revised as below suggestion.

We greatly thank the reviewer for his/her careful reading of our manuscript and the supportive comments. We address the referee's specific comments as below. Please check the highlighted sentences in the revised manuscript for those changes.

Specific comments：

1. Line 20, please reconfirm the dust storm date of "March 19-27" is right. I think it should be "March 19-23".

Thanks for pointing out this typo. The dust storm date is from March 19-23 and it is corrected in the revised version as "Near surface and vertical in situ measurements of atmospheric particles were conducted in Shanghai during March 19-23, 2010 to explore the transport and chemical evolution of dust particles in a super dust storm."

2. Line 124, same to the question above.

The dust storm date is from March 19-23, but the TSP samples in this study were collected from March 19-27, including the dust days and the non-dust days after the dust episodes. Thus, the date in Line 124 is correct.

3.Line 163. How get the Chigh and Clow to calculate the C? It seems that you can derive the Ihigh and Ilow from the API grading limited value table according your description. Can you derive the ihigh and Ilow directly from the table?

Thanks for the comments. In China, six grades of air pollution of excellent, good, slightly polluted, lightly polluted, moderately polluted, and heavily polluted were set corresponding to the API scales of 0-50, 51-100, 101-150, 151-200, 201-300, and >300, respectively. Both API values of 50, 100, 200, 300, 400, and 500 and their corresponding concentrations of air pollutants were defined in the API grading limited value table as shown in Table S1. According to the definition of API in China, the API value of air pollutants was calculated as $I = (I_{high} - I_{low})(C - C_{low})/(C_{high} - C_{low}) + I_{low}$, where C and I are the concentration and the API value of a specific air pollutant, respectively. I_{high} and I_{low} stand for the two values in the API grading limited value table that mostly approach to value I, respectively. C_{high} and C_{low} represent the concentrations corresponding to I_{high} and I_{low}, respectively. Thus, once getting the API

value of PM_{10}, it can be converted to PM_{10} concentration as $C = (I - I_{low})(C_{high} - C_{low})/(I_{high} - I_{low}) + C_{low}$.

Table S1. The API grading limited value and the corresponding concentrations of air pollutants in China (Ministry of Environmental Protection of the People's Republic of China, Technical requirements for urban ambient air quality daily report and forecast, 2008, http://www.zhb.gov.cn/gkml/hbb/bgth/200910/t20091022_174917.htm).

API	Concentration（μg/m^3）*				
	SO_2	NO_2	PM_{10}	CO	O_3
50	50	80	50	5000	120
100	150	120	150	10000	200
200	800	280	350	60000	400
300	1600	565	420	90000	800
400	2100	750	500	120000	1000
500	2620	940	600	150000	1200

*24h average concentrations for SO_2, NO_2, PM_{10}, and CO and 8h average concentrations for O_3

We have revised Section 2.3 as below.

Air pollution index (API) data in 86 major cities (locations shown in Fig. 1a) over China were obtained from the data center of Ministry of Environmental Protection of China (http://datacenter.mep.gov.cn/). In China, six grades of air pollution of excellent, good, slightly polluted, lightly polluted, moderately polluted, and heavily polluted were set corresponding to the API scales of 0-50, 51-100, 101-150, 151-200, 201-300, and >300, respectively. Both API values of 50, 100, 200, 300, 400, and 500 and their corresponding concentrations of air pollutants were defined in the API grading limited value table as shown in Table S1. According to the definition of API in China, the API value of air pollutants is calculated as $I_x = (I_{x,\,high} - I_{x,\,low})(C_x - C_{x,\,low})/(C_{x,\,high} - C_{x,\,low}) + I_{x,\,low}$, where C_x and I_x are the concentration and the API value of air pollutant X in Table S1, respectively. $I_{x,\,high}$ and $I_{x,\,low}$ stand for the two values in the API grading limited value table that mostly approach to value I_x, respectively. $C_{x,\,high}$ and $C_{x,\,low}$ represent the concentration of X corresponding to $I_{x,\,high}$ and $I_{x,\,low}$, respectively. And the daily API value is defined as $API = Max(I_{PM10}, I_{SO2}, I_{NO2}, I_{CO}, I_{O3})$. According to API data records from March 20 to 23, 2010, PM_{10} was the premier air pollutant in most of the 86 cities over China, i.e. $API = I_{PM10}$. Thus, the API value can be converted to PM_{10} concentration as $C = (I - I_{low})(C_{high} - C_{low})/(I_{high} - I_{low}) + C_{low}$. It should be noted that API was recorded with a maximum value of 500, which corresponded to the PM_{10} concentration of 600 μgm^{-3}.

4. Figure 3, please add the description of the x axis that if it is local time or UTC, it

sometimes make me confused.

Thanks for the suggestion. Local time is used in this study. It is now indicated clearly in the caption of Figure 3.

5. Figure 4, I suggest that you can add the direction of north to south and east to west to give a clear direction of the wind.

Thanks for the suggestion. Figure 4 is revised as below.

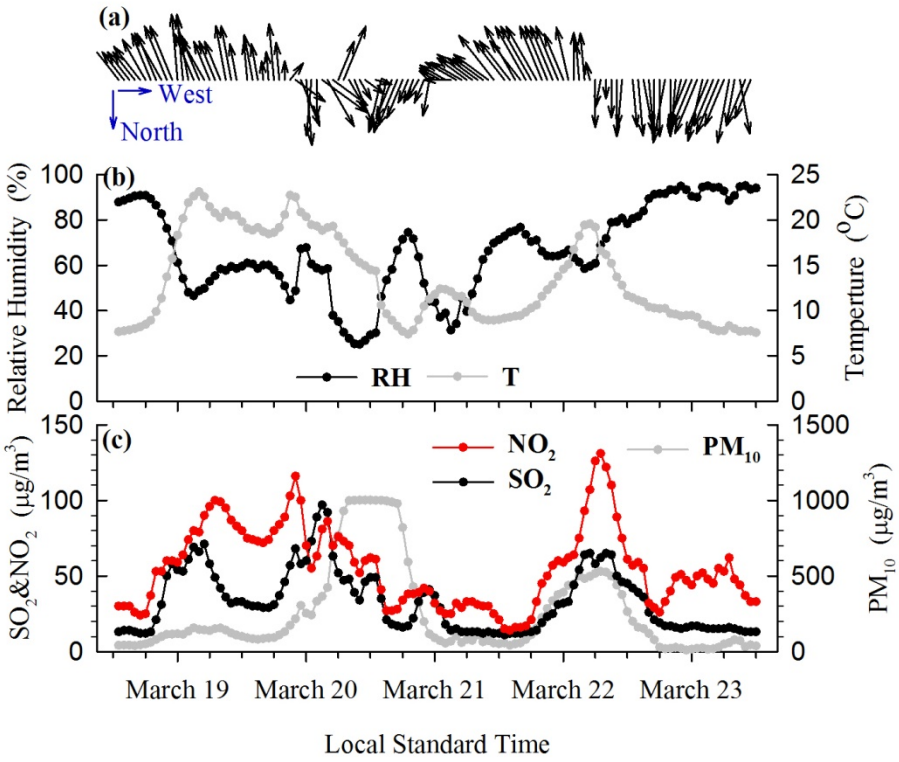

6. Line 288, in Fig. 4c there are obviously decrease of NO2 and SO2 before they increase to the maximum during 6-18 on March 19.

Thanks for the comment. As shown in Fig. 4c, the concentrations of NO_2 and SO_2 indeed synchronously decreased before their maximum. This was partly attributed to the prevailing southeast winds, i.e. sea breezes which had clean effects on the local pollution. Furthermore, the decrease of NO_2 and SO_2 occurred during night from 18 LST of March 19 to 6 LST of March 20, when the anthropogenic emissions were relatively low during a day.

The related paragraph is revised as below.

As shown in Fig. 4a, the winds prevailed from the south before the onset of DS1 at ~10:00LST, March 20. Starting from early morning of March 19, SO_2 and NO_2 continuously climbed up due to the enhanced human activities. From 18:00 LST of

March 19 to 6:00 LST of March 20, the concentrations of NO_2 and SO_2 synchronously decreased. This was partly attributed to the prevailing southeast winds, i.e. sea breezes which had clean effects on the local pollution. Furthermore, the decrease of NO_2 and SO_2 occurred during night, when the anthropogenic emissions were relatively low during a day. During this period, SO_2 and NO_2 concentrations were relatively high with mean concentrations of 39 ± 19 and $70 \pm 25 \mu gm^{-3}$, respectively.

7. Line 389, why the number of Ca2+ in DS1 is larger than that in DS1, although the intensity of DS1 was much stronger than DS2?

Thanks for the comment. The abundance of Ca^{2+} during the dust episodes depended on both the intensity of dust and the reaction efficiency of the insoluble $CaCO_3$ to the soluble Ca^{2+}. Although the intensity of DS1 was much stronger than DS2, the concentrations of Ca^{2+} in DS2 were comparable to that in DS1 (Fig. 6b), while the mass ratios of Ca^{2+} in TSP were even higher in DS2 than in DS1 (Fig. 6d). This was mainly attributed to that more calcium in its soluble form (e.g. $Ca(NO_3)_2$ and $CaSO_4$) was produced via the reactions between calcium carbonate and acids. Particularly, higher concentrations and mass ratios of NO_3^- in TSP in DS2 were observed than in DS1 (Fig. 6a&c), indicating more $Ca(NO_3)_2$ was formed in DS2 than in DS1. Moreover, the ratio of Ca^{2+}/Ca was higher in DS2 (0.2-0.5) than in DS1 (0.1-0.2) (Fig.7a), indicating a higher fraction of calcium carbonate from dust particles was transformed to soluble calcium.

8. Line 465, I suppose the ratio of "[NH4++Ca2+]/[SO42-+NO3-]" should be change into "[NH4++Ca2++Mg2+]: : :" as Fig.7 shows.

Thanks for pointing out this. It should be $[NH_4^+ + Ca^{2+} + Mg^{2+}]/[SO_4^{2-} + NO_3^-]$ in Line 465.

In the revised version Line 465-472 was corrected as "We further investigated the $[NH_4^+ + Ca^{2+} + Mg^{2+}]/[SO_4^{2-} + NO_3^-]$ ratio. As shown in Fig. 7d, with the addition of Ca^{2+} and Mg^{2+}, sulfate and nitrate had been completely neutralized, implying the important role of alkaline calcium and magnesium as the medium of dust heterogeneous reactions. By estimating the neutralization efficiency of Ca^{2+} and Mg^{2+} ($NE_{Ca\&Mg}$) as $NE_{Ca\&Mg} = 1 - [NH_4^+]/[SO_4^{2-} + NO_3^-]$, the average value of $NE_{Ca\&Mg}$ in DS1 and DS2 was 0.34 and 0.50, respectively. The higher $NE_{Ca\&Mg}$ in DS2 also suggested the chemical processing via dust was efficient under the environmental conditions such as DS2 in this study."

9. Line, 576, from the Fig. 9d, I also see there is a high mineral aerosols center at Gobi Desert, but the satellite can't show the same phenomenon. Please explain it.

Thanks for pointing out this. As the satellite data is at daily resolution, the missing values of OMI Aerosol Index shown in the figure were mainly due to the gaps between the satellite swaths. If the swath width didn't cover the Gobi Desert, e.g. on

March 20 & 22, high spots of OMI Aerosol Index were not shown over the target region. When the satellite swath passed over the Gobi Desert on March 21, we did see high values of Aerosol Index over the Mongolian Gobi Desert and this was relatively consistent with the mineral dust simulation.
However, based on the definition of Aerosol Index, it is a parameter based on the difference between radiance at two near ultraviolet wavelengths. Thus, the comparison between satellite Aerosol Index and simulated mineral dust is only qualitative.
In the revised manuscript, we have indicated this in the second paragraph of Section 3.6.

10. I would recommend the authors include and discuss these studies about dust transport over East Asia especially in March 2010 in the introduction.
Thanks for the suggestion. We have included and discussed these studies in the introduction in the revised version.

Asian dust originating from the arid and semiarid areas in Mongolia and China can be transported for long distances, reaching Beijing (Sun et al., 2010), Shanghai (Fu et al., 2010), Xiamen (Zhao et al., 2011), Taiwan (Tsai et al., 2012; Tsai et al., 2014), and even as far as North America (Uno et al., 2009; Wu et al., 2015), exerting significant impacts on the air quality of both densely populated habitations and remote regions. Huang et al. (2014) showed that Asian dust could transport from the Qilian Mountain or from the Qaidam Basin through Qinghai and Gansu provinces to reach the Pacific Ocean, and that dust originating from the Taklimakan Desert could travel across the Hexi Corridor and Loess Plateau to reach southeastern China. Zhao et al. (2009) demonstrated that the deserts in Mongolia and in western and northern China were the major sources of Asian dust particles in East Asia and estimated that 26% of the dust particles emitted from Asian dust sources was transported to the Pacific Ocean. Eguchi et al. (2009) reported that the dust plume from the Gobi Desert in East Asia was transported at low altitudes of 4-6km to North America and mixed with Asian anthropogenic air pollutants during its transport. Fu et al. (2014) simulated that during a dust event from May 1 to 6, 2011, the transported dust particles accounted for 78.9% of the surface layer PM_{10} over the Yangtze River Delta.

Dust aerosols can significantly influence the regional/global climate directly by absorbing and scattering solar radiation (Bi et al., 2016) and also indirectly by influencing the formation of ice nuclei, cloud, and precipitation (Creamean et al., 2013; Li and Min, 2010; Wang et al., 2010). In addition, deposition of transported dust aerosols into the ocean can enhance phytoplankton blooms due to the existence of bioavailable iron (Wang et al., 2012; Zhuang et al., 1992), which indirectly impacts on global climate change. The effects of dust aerosols on climate change depend critically on their physical and chemical properties. Natural dust aerosols with limited contamination have low light-absorption, with single-scattering albedo of 0.91-0.97 at 500nm and 550nm (Bi et al., 2014; Uchiyama et al., 2005). During the long-range transport, dust aerosols are often modified by their mixing with anthropogenic emissions over the downwind areas (Fischer et al., 2011; Formenti et al., 2011; Huang

et al., 2010b; Tobo et al., 2010), resulting in high uncertainties in evaluating the climatic effects of dust aerosols. It was estimated that mineral dust had a radiative forcing of -0.1±0.2 Wm^{-2} (IPCC, 2013), of which the uncertainty was as high as 200%. Obviously, the characteristics of dust particles and their evolution during the transport are not well understood.

In March 2010, a super dust storm swept China, invading extensive areas from Northern China to Southern China including Fujian and Guangdong provinces, and lasting for ~4 days from March 19 to 23 (Li et al., 2011). The dust plumes further extended to the South China Sea (Wang et al., 2011), Taiwan (Tsai et al., 2013), Korea (Tatarov et al., 2012), Japan (Zaizen et al., 2014), and even to North America (Wu et 70 al., 2015). This dust storm was as strong as the one in March 20-21, 2002 and attracted considerable attentions. Chen et al. (2017) used WRF-Chem to simulate the emission and transport of dust particles over the Taklimakan Desert and Gobi Desert. The results indicated that the Gobi Desert dust particles were easily lifted to 4km and subject to the long-range transport, which contributed much more to the dust plumes over East Asia than the Taklimakan Desert dust. Lidar observations revealed that this super dust storm was transported within a low altitude (Tatarov et al., 2012; Wang et al., 2011), which could benefit the mixing and interaction between dust particles and anthropogenic pollutants. Indeed, modifications of dust particles during the transport of this dust storm were suggested based on in situ measurements. Zhao et al. (2011) displayed substantial increases of particulate sulfate and nitrate when the dust plumes arrived at Xiamen city of Fujian province, implying the mixing and interaction between dust particles and anthropogenic pollutants. Wang et al. (2011) indicated that the dust particles detected at the Dongshan Island over the South China Sea were mixed with anthropogenic and marine particles. Observations of this dust storm at Tsukuba and Mt. Haruna, Japan showed that most of the transported dust particles in lower altitudes were internally mixed with sulfate or seasalt (Zaizen et al., 2014).

References:

Zhao, T.L., S. L. Gong, X. Y. Zhang, et al., 2006: A Simulated Climatology of Asian Dust Aerosol and Its Trans-Pacific Transport. Part I: Mean Climate and Validation. J. Climate., 19,88–103. doi: http://dx.doi.org/10.1175/JCLI3605.1.

Eguchi, K., I. Uno, K. Yumimoto, et al., 2009: Trans-pacific dust transport: integrated analysis of NASA/CALIPSO and a global aerosol transport model. Atmos. Chem. Phys., 9, 3137-3145.

Fu,X., S. X. Wang, Z. Cheng, J. Xing, B. Zhao , J. D. Wang, and J. M. Hao, 2014: Source, transport and impacts of a heavy dust event in the Yangtze River Delta, China, in 2011. Atmos. Chem. Phys., 14, 1239–1254.

Huang J., T. Wang, W. Wang, Z. Li, and H. Yan, 2014: Climate effects of dust aerosols over East Asian arid and semiarid regions. J. Geophys. Res.: Atmospheres, 119, 11398-11416.

Chen S., J. Huang, L. Kang, H. Wang, X. Ma, Y. He, T. Yuan, B. Yang, Z. Huang, and G. Zhang (2017). Emission, transport and radiative effects of mineral dust from Taklimakan and Gobi Deserts: comparison of measurements and model results. Atmospheric Chemistry and Physics,17(3):1-43, doi: 10.5194/acp-17-2401-2017.

Response to Comments from Anonymous Referee #2

The paper describes an interesting case study on interaction between dust and air pollution. The measurements of water-soluble ions showing heterogeneous reactions are especially interesting. I feel the subject is similar to that described in Pan et al., recently, though the observation methods are different. Pan et al. showed the change in morphology of dust by interaction with air pollution in Beijing (Pan et al., 2017, Real-time observational evidence of changing Asian dust morphology with the mixing of heavy anthropogenic pollution, Scientific Reports 7, 335, doi:10.1038/s41598-017-00444-w). I think it would be better to cite the paper and give a discussion.

We thank the reviewer for his/her careful reading of our manuscript and the supportive comments. We address the referee's specific comments as below. Please check the highlighted sentences in the revised manuscript for those changes.

The paper (Pan et al., 2017) recommended by the reviewer is now cited and discussed in the revision as "(Line 434) …due to the heterogeneous reactions. Recently, Pan et al. (2017) reported that the concentrations of both NO_3^- and Ca^{2+} increased in coarse mode mineral dust in Beijing, particularly at high RH condition due to the interaction between nitric acid and Ca-rich particles. It is further suggested that the impact of nitrate on modifying the morphology of dust particles have become increasingly important, as the NOx emissions in East Asia have been rapidly increasing."

1. What is the definition of the depolarization ratio (DR)? Is it volume depolarization ratio (total depolarization ratio)? or particle depolarization ratio (aerosol depolarization ratio)? They are different and should not be confused. Depolarization ratio shown in Fig. 3 is probably volume depolarization ratio (including molecular scattering), but the particle depolarization ratio must be used in the analysis for partitioning dust and non-dust particles.

Thanks for pointing out this issue. The depolarization ratio shown in Fig. 3 is indeed volume depolarization ratio (δv), which is used to qualitatively identify the occurrence of dust events. When partitioning dust from non-dust particles, the particle depolarization ratio (δp) has been applied. In the revised manuscript, δv and δp are clearly defined.

The first paragraph in Section 3.2 is revised as "Fig. 3a shows the time-height cross-section of δv (volume depolarization ratio) measured at the wavelength of 532 nm from March 19 to 23 in Shanghai. δv is frequently used to identify dust events and a threshold value of 10% is used to distinguish dust from other types of particles (Shimizu et al., 2004). As shown in Fig. 3a, there were evidently two discontinuous periods with δv higher than 10%, consistent with the two peaks of PM_{10} concentrations measured near the ground (Fig. 4c). The first dust episode (DS1) started from ~16:00 LST, March 20 to ~10:00LST, March 21 and the second dust

episode (DS2) started from ~6:00 LST, March 22 to ~0:00 LST, March 23."

2. Is the measured volume depolarization ratio calibrated? It is essential if the authors discuss the value of the particle depolarization ratio. It is also essential for partitioning dust and non-dust.

Thanks for the comment. Yes, the observed signals used to calculate volume depolarization ratio (δv) have been calibrated before the calculation. Briefly, a sheet polarizer with the polarizing direction set at 45 degree (then -45 degree) to the polarizing plane of the emitted light was installed in front of the beam splitter cube, and two sets of backscatter signal profiles from the sky were obtained for the calibration. Detailed calibration procedure has been described in Shimizu et al. (2004) and Shimizu et al. (2017).

Section 2.1.1 is revised as "A dual-wavelength depolarization Lidar (Model:L2S-SMII) developed by the National Institute for Environmental Studies (NIES) of Japan was installed on the roof (~20m above ground level) of a teaching building on the campus of Fudan University in the Yangpu District of Shanghai (Fig. 1b). The Lidar measurement was performed every 15 min (at 00, 15, 30, and 45 minutes every hour) with a height resolution of 6 m. Attenuated backscattering coefficient (β), volume depolarization ratio (δv), particle depolarization ratio (δp), and particle extinction coefficient (σ) at the wavelength of 532 nm were obtained by the measurement. More details about the Lidar system have been described in Huang et al. (2012). δv is calculated using the parallel (Ip) and perpendicular (Is) components of backscatter intensity, and Ip and Is were calibrated before the calculation. Briefly, a sheet polarizer with the polarizing direction set at 45 degree (then -45 degree) to the polarizing plane of the emitted light was installed in front of the beam splitter cube, and two sets of backscatter signal profiles from the sky were obtained for the calibration. Detailed calibration procedure has been described in Shimizu et al. (2004) and Shimizu et al. (2017). σ was derived by the Fernald inversion method (Fernald, 1984) with the lidar ratio (extinction-to-backscatter ratio) set as 50 sr (Liu et al., 2002) in the inversion process. The total aerosol extinction coefficient can be split to non-spherical particle (dust particle, σ_d) and spherical particle (mostly pollution particle, σ_s) fractions based on the value of δp. The splitting method has been described in detail by Sugimoto et al. (2002) and Shimizu et al. (2004).

To solve the problem that overlap of the laser beam and the view field of telescope is insufficient for near surface observation, a compensation function Y(z) was applied. Function Y(z) was derived from the signal profiles that observed on a day when the planetary boundary layer was well developed. With the compensation, the optical properties of the particles above 120 m altitude were provided. Detailed correction procedure has been described in Shimizu et al. (2017)."

3. Is the correction to the geometrical form factor (overlap function) applied? The decrease of the extinction coefficient near the surface in Fig. 8 seems not true. The

correction should be applied if not. Unreliable part of the figure should be masked at least.

Thanks for the comment. To solve the problem that overlap of the laser beam and the view field of telescope is insufficient for near surface observation, a compensation function Y(z) was applied. Function Y(z) was derived from the signal profiles that observed on a day when the planetary boundary layer was well developed. With the compensation, the optical properties of the particles above 120 m altitude were provided. Detailed correction procedure has been described in Shimizu et al. (2017).

The vertical profiles shown in Fig. 8 have been revised starting from the altitude of 150 m, with unreliable data below 150 m excluded as suggested.

We have added this paragraph in Section 2.1.1 as shown above in last specific comment.

4. What is reason to show attenuated backscattering coefficient (BSC) in Fig. 8? It doesn't make sense to me. Dust extinction coefficient, non-dust extinction coefficient, and total extinction coefficient (dust + non-dust) should be indicated in the upper panels. The depolarization ratio in the lower panels must be the particle depolarization ratio.

Thanks for the comment. Fig. 8 is revised as suggested that the attenuated backscattering coefficient is replaced by the total extinction coefficient and the particle depolarization ratio is used in the lower panels.

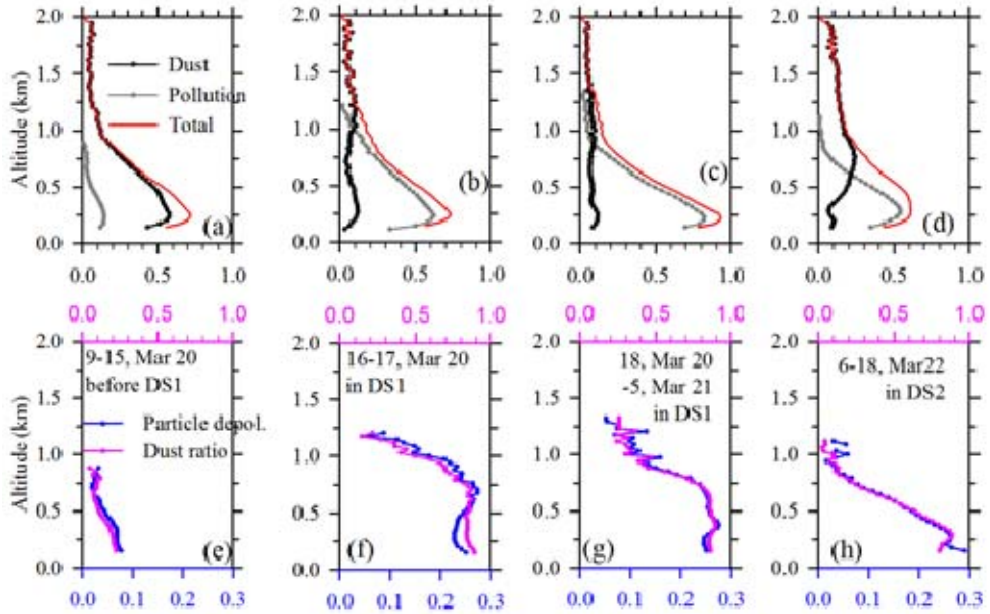

Fig.8 Vertical profiles of the average extinction coefficients of dust, pollution, and total particles (km^{-1}), particle depolarization ratios (Particle depol., unitless), and the ratio of the dust extinction in the total extinction (Dust ratio, unitless) in four periods of 9:00 - 15:00 of March 20 (before DS1), 16:00 - 17:45 of March 20 (before the highest PM_{10} concentration in DS1), 18:00 of March 20 - 04:45 of March 21 (during the highest PM_{10} concentration in DS1), and 6:00 - 18:00 of March 22 in DS2.